Analyst

ROYAL SOCIETY OF CHEMISTRY

PAPER

View Article Online
View Journal | View Issue

Cite this: *Analyst*, 2025, **150**, 3690

A minimal sampling, in-line spectroscopic calibration method for unstable components during ammoniation of fatty acids†

C. M. Raffel,[a] J. Meekes,[b] H.-J. van Manen,[b] A. J. B. ten Kate,[b] A. Chaudhuri[a] and J. van der Schaaf *[a]

The ammoniation of fatty acid produces fatty amide, as well as unstable ammonium salt, whose composition profile can vary with off-line sampling. This makes the analysis and determination of reaction kinetics challenging. In-line FT-IR spectroscopy removes the need for sampling, but requires calibration of the reacting system at reaction conditions, which is complicated by the near-instant formation of ammonium salt. In this work, we demonstrate the development of a calibration method which overcomes the complexities posed by both off-line and in-line analysis. This is achieved by taking only eight off-line samples for determination of the more stable components and formulating mass balances of the reactive system for each in-line acquired FT-IR spectrum. This allows for the determination of the rapidly fluctuating salt content. The essential assumptions underlying the mass balances and the resulting calibration are based on a qualitative examination of the reaction system through principal component analysis. Put together, this enables in-line calibration of the system at reaction conditions, achieving relative errors below 10% using partial least squares regression.

Received 1st August 2024,
Accepted 2nd June 2025

DOI: 10.1039/d4an01051e

rsc.li/analyst

1 Introduction

The production of base chemicals from renewable resources is of critical concern in the future to reduce the need for fossil-based feedstocks. The production of fatty amides from fatty acids, traditionally sourced from waste plant oil or animal fat, is the perfect embodiment of such a sustainable manufacturing strategy. These fatty amide compounds are an important class of base chemicals mainly used as lubricants[1–3] and in the production of fatty amines, as well as in the production of several types of fatty amine based surfactants.[4–6]

Fatty acid reacts with ammonia to fatty amide and water in an equilibrium reaction, where at higher temperatures of about 250 °C, the fatty amide dehydrates further to give the fatty nitrile,[7] usually further accelerated by using a metal oxide catalyst.[7,8] At lower temperatures, the fatty acid can also react with ammonia in an acid–base reaction to form the fatty acid ammonium salt.[9] The possible reactions of fatty acid with ammonia are illustrated in Fig. 1.

There is some debate in literature concerning the reaction mechanism for the amide formation, where the ammonium salt formation is sometimes considered to be a reaction intermediate between the acid and the amide reaction step,[7,10] while other researchers have also proposed it to be a side reaction.[9,11] In this work, the formation of ammonium salt is represented as a side reaction as shown in Fig. 1, following the findings suggested by Charville *et al.*[11] A possible reason for the debate can be the relative instability of the ammonium salt: while the fatty acid sodium salt precipitates as a solid with a high decomposition temperature, the ammonium salt is readily transformed back to acid and ammonia.[9] The formation of ammonium salt is exothermic and disfavored at

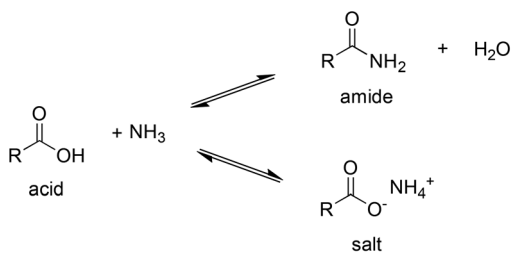

Fig. 1 General reaction scheme for the production of fatty amides from fatty acid. R corresponds to a largely saturated hydrocarbon chain with 8–22 carbon atoms, potentially with one ore more double bonds.

[a]*Laboratory of Chemical Reactor Engineering, Department of Chemical Engineering and Chemistry, Eindhoven University of Technology, P.O. Box 513, 5600 MB Eindhoven, The Netherlands. E-mail: j.vanderschaaf@TUE.NL*
[b]*Nouryon Specialty Chemicals, Zutphenseweg 10, P.O. Box 10, 7400AA Deventer, The Netherlands*

†Electronic supplementary information (ESI) available. See DOI: https://doi.org/10.1039/d4an01051e

elevated temperatures. For instance, Bizhanov *et al.* observed only up to 2 mol% at 300 °C with titration.[10]

The rapid formation and decomposition of the ammonium salt depending on the readily shifting acid–base equilibrium complicates the analysis of the reaction mixture and consequently the development of mechanistic and kinetic models of the reaction, which are necessary to enable process improvement. As the ammonium salt is unstable, especially compared with the more stable amide, it is likely highly dependent on the ammonia pressure in the reactor, which is itself a function of temperature. Withdrawing a sample from a reactor containing ammonia at reaction conditions, and thereby reducing temperature and pressure, will quickly shift the acid–base equilibrium. This of course will have implications on the ammonium salt composition, as it can then decompose to give fatty acid and ammonia in *ex situ* samples. Along with providing possible erroneous sample composition, *ex situ* measurements can also lead to safety issues due to ammonia flashing from the sample into the air.

An elegant solution to this issue would be to switch from off-line analysis to an in-line technique, for instance FT-IR spectroscopy. In-line analysis allows real-time monitoring of the reaction, measuring a new data point every few seconds. It is a safe and non-invasive measurement technique, where the measurement probe is installed in the reactor and no sampling is required. The reaction equilibria are not altered by removal from the reaction temperature and pressure, and the stability of the sample is no issue. Furthermore, the amount of data gathered in a single experiment is significantly greater for in-line analysis than off-line sampling.[12–14] However, calibration of the in-line spectroscopic system is complicated by the unknown and changing composition of the reaction mixture. The calibration has to be carried out at reaction temperature, as temperature affects IR spectra. Thus, a calibration carried out at room temperature may not be valid at reaction temperature. Even at milder reaction temperatures such as 120 °C, ammonium salt is reactive. It can easily decompose to the acid, and while the reaction to amide is still slow at these temperatures, amide also forms, as we illustrate in this study. Therefore, while the FT-IR calibration has to be carried out in-line at reaction temperature, it needs to take into account the reaction occuring during this calibration. To be able to do so, assumptions have to be formulated based on a deeper understanding of the reactive system and the reactions and equilibria governing it.

This work aims to study the ammoniation of fatty acid to ammonium salt and to fatty amide at 120 °C with in-line FT-IR spectroscopy. We present an in-line calibration method of the reactive system at reaction conditions to quantify acid, amide and salt in the reaction mixture. This is achieved by first gaining a deeper understanding of the reactive system through qualitative chemometric analysis of the reaction with principal component analysis (PCA) applied to the FT-IR spectra. This allows us to formulate assumptions which are used to perform the in-line calibration at reaction conditions, whose predictive capabilities are subsequently validated experimentally. The experimental approach followed in this study can also be widely applied to similar reactive systems where in-line measurements can provide an added advantage.

2 Methods

2.1 Experimental

Purified oleic acid (75% oleic acid (C18 : 1), linoleic acid (C18 : 2) 12%, palmitic acid (C16) 2%, stearic acid (C18) 2%) from VWR and water-free ammonia (pure, Gerling Holz & Co.) were used for the reaction. Oleic amide (>65%, TCI, impurities mostly amides of other chain lengths) was used in combination with oleic acid for the binary experiments. Sodium oleate, the sodium salt of oleic acid (>97%, TCI) was used for recording a pure component IR spectrum of an oleic acid salt, as no pure ammonium oleate was available commercially.

A 3 L stainless-steel batch reactor (Büchi, type 4, with baffles) with a custom-made flange on the reactor side was used for the experiments as illustrated in Fig. 2. The single-bounce ATR probe with diamond crystal (9.5 mm AgX DiComp) of the FT-IR spectrometer (ReactIR 15, Mettler-Toledo) was inserted through the flange into the reactor so that it would be covered by the reaction liquid at all times. The reactor was stirred at 500 rpm. With calculated mixing times below 0.5 s in the turbulent regime, uniform mixing within the reactor was assumed over the course of the hours-long experiments. It was ensured that the probe position had no effect on the measurements. Before starting an experiment, the fatty acid in the reactor was deaerated by purging with nitrogen. To start the experiment, ammonia was fed *via* a Bronkhorst mass flow meter and controlled with a flow control valve (Badger) at pressures up to 8 bar through a dip tube, ensuring good gas–liquid contacting. The reactor temperature was controlled at 120 °C during all experiments. The pressure in the reactor headspace – which built up slightly due to the formation of water – was logged during all experiments. Physical samples for off-line analysis of the reaction mixture were taken from the bottom of the reactor.

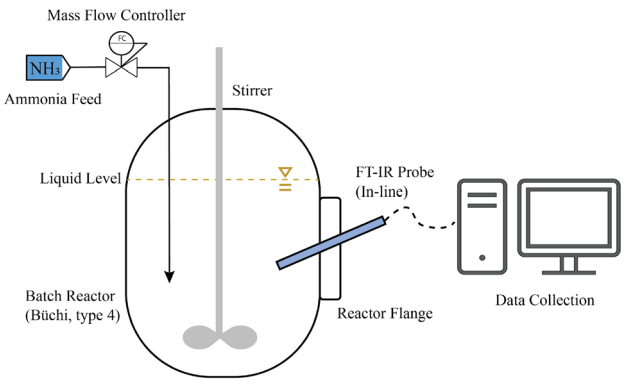

Fig. 2 Set-up for in-line measurement of oleic acid ammoniation.

Analysis of the off-line samples was carried out with GC-FID (Shimadzu GC-2010 Plus) with a 30 m dimethyl polysiloxane column (Shimadzu, SH-Rtx-1, 0.32 mm ID). 100 mg of the sample was dissolved in 1 mL of 2-propanol (98%, Boom Laboratoriumleverancier). The oven temperature was ramped from 150 °C to 250 °C over 10 min and kept constant at 250 °C for 15 min. This GC-analysis allows to separate amide and acid, however, all ammonium salt present in the sample reverts back to acid, which means the measured acid fraction is the sum of salt and acid present in the sample. The amide content can be reliably determined with this method (see ESI, Table S2†). The pure component FT-IR spectra of oleic acid, oleic amide and sodium oleate were measured off-line at room temperature with a Thermo Scientific iS50 ATR instrument.

2.1.1 Experimental procedure. All reactions were monitored with the FT-IR spectrometer, which recorded a new spectrum every 16 s with a resolution of 2 cm^{-1}. A background spectrum was taken before every experiment in an empty reactor flushed with nitrogen.

Experiments with the reactive mixture and ammonia were performed starting from pure oleic acid. One experiment was performed for calibration, and one with a similar procedure for validation of the calibration. For both experiments, 2 kg of oleic acid were added to the reactor and heated while purging with nitrogen to remove any water dissolved in the system. Once 120 °C was reached, nitrogen was shut off and the reactor was closed, the reactor was at a starting pressure of 1 atm.

2.1.1.1 Calibration experiment. To the 2 kg of oleic acid at 120 °C, 7 g of ammonia were added with a feed rate of 1.05 g min^{-1}. This feed rate was chosen as it led to no temperature rise during ammonia dosing from the exothermic salt formation and the temperature of the reactor stayed stable at 120 °C. After the dosing of ammonia, the mixture was left to react without addition of any ammonia or taking of samples, this will subsequently be called a "reaction plateau". The length of these plateaus varied from 20 min to 40 min. At the end of a reaction plateau, a sample was taken from the reactor for off-line-analysis and determination of the amide content. Directly after taking a sample, the next ammonia dosing step was started. The first six dosing steps dosed 7 g of ammonia each, the seventh 14 g and the eighth 21 g, so that at the end of the experiment, 77 g of ammonia had been dosed in total, which corresponds to 75 mol% of the initial 2 kg of oleic acid.

The composition of the liquid samples taken could be calculated from the off-line GC-analysis and an ammonia mass balance, and related to the in-line FT-IR spectrum taken at the time of sampling. The calculation method for the eight samples taken is explained for the first sample. The assumptions made for this calculation are justified in subsection 3.2 and are not covered in detail in this section. At the time t_1 that the first sample was taken, the information shown in Table 1 on the reaction mixture is available, where $n_{acid,init}$ is the initial amount of oleic acid added to the reactor, m_{NH_3} is the amount of ammonia added at the time t_1 and x_{amide} was measured from the off-line sample.

Table 1 Measurable information on reactor content at time of first sample

Time of sample 1	$n_{acid,init}$ [mol]	m_{NH_3} in reactor [g]	x_{amide} [–]
t_1	7.005	7.05	0.006

Assuming that all ammonia added to the reactor has reacted with acid (see subsection 3.2), it will either react to amide or to salt. The acid content in sample 1 is then

$$n_{acid,i} = n_{acid,init} - n_{NH_3,i} \quad (1)$$

with $i = 1$. The rest of the acid has reacted. The amount that reacted to amide was measured with GC, so the amount of salt in sample 1 is calculated with ($i = 1$)

$$n_{salt,i} = n_{acid,init} - n_{acid,i} - n_{amide,i} \quad (2)$$

The composition of the other seven samples can be calculated accordingly for $i = 2,\ldots,8$. An overview of the sample composition is given in the ESI (Table S3†).

2.1.1.2 Validation experiment. To validate the calibration performed, a similar experimental procedure was carried out. Now, 77 g of ammonia was dosed in nine dosing steps instead of eight, and only one off-line sample was taken after the last dosing step. The salt and amide composition was measured only for this single sample. For the rest of the samples, the acid content can be determined from eqn (1).

2.2 Analysis of FT-IR spectra

The raw spectra collected during the experiments were further processed using PLS_Toolbox Version 8.8.1 (Eigenvector Research, Inc.) running under Matlab R2018b (The MathWorks). PLS_Toolbox is able to visualize the several hundred spectra collected during the experiments. Different chemometric analyses can be performed with this program as well, such as principal component analysis (PCA) and partial least squares (PLS) analysis.

The raw FT-IR spectra collected during reaction were measured at wavelengths from 4000–650 cm^{-1}, though mostly noise was measured from 4000–3000 cm^{-1} due to instrumental limitations. The spectra of acid, amide and salt show the most variation in the spectral range of 1820–950 cm^{-1}, so only data in this spectral range was considered for further analysis. To prepare the raw spectra for chemometrical analysis, different pre-processing methods were applied to the spectra. The pre-processing methods for each specific analysis are specified during their discussion in section 3.

3 Results and discussion

3.1 General calibration strategy

The general approach for the calibration procedure developed in this work is covered in this section. An important first step is to identify and assign the IR bands characteristic for the reaction system.

3.1.1 Band assignment. The position of the characteristic bands of the pure components of acid, amide and salt were measured off-line at room temperature, shown in an overlay in Fig. 3. As no pure ammonium salt was available due to its instability, sodium salt was used, as the position of the COO^- band is not influenced by the salt counter ion.[15,16]

Now, the characteristic C=O stretch vibration of the carboxylic acid dimer is at a wavenumber position of 1710 cm^{-1} and that of the carboxylic acid monomer at 1750 cm^{-1} (nearly invisible at room temperature[17]).[18] The oleic amide has two characteristic peaks, the C=O stretch vibration at 1650 cm^{-1} and the N–H deformation at 1620 cm^{-1}.[19,20] The COO^- asymmetric stretch vibration of the sodium or ammonium oleate is at 1550 cm^{-1}.[16] The characteristic peaks of the pure components are close together and slightly overlap, but are separate and identifiable.

3.1.2 Calibration with an unstable component. With the characteristic bands of the pure components identified, the next step is to develop a calibration strategy, an overview of which can be seen in Fig. 4, and explained further below.

An intuitive approach to calibration is to measure mixtures of known concentrations of the pure components. These are acid, amide and salt, as the concentrations of water and ammonia are negligible in the system, as will be shown in subsubsection 3.2.1. With proper safety measures it was possible to withdraw eight samples from the system. However, as the salt is unstable and readily converts to acid and ammonia, the only compound reliably quantifiable in these samples is the more stable amide. Measuring mixtures of acid, amide and salt at 120 °C in the reactor leads to reaction, as the salt can decompose to acid and ammonia and form amide and water. Thus, the presence of the unstable component has to inform the calibration strategy. One approach is to perform the calibration for an unreactive partial system and extrapolate to the complete, reactive system. At 120 °C, acid and amide do not react significantly, so performing a calibration for the binary system is possible, as shown in the ESI S1.† However, the extrapolation from this calibration to the reactive system containing salt proved impossible as the presence of salt changes the spectra significantly. The salt band is close to the amide bands as seen in Fig. 3 and slightly overlaps with them. Therefore a calibration of the three components has to be carried out in the reactive system by dosing ammonia leading to *in situ* salt formation.

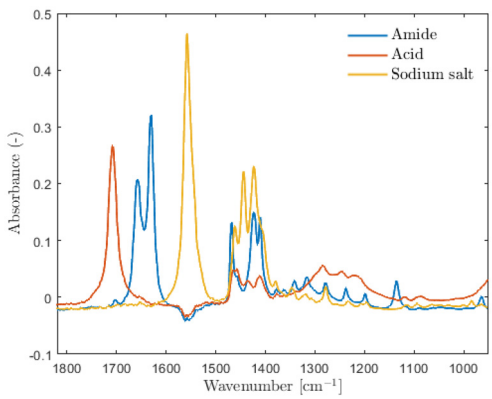

Fig. 3 Pure component spectra of oleic acid, oleic amide and sodium oleate at room temperature in the relevant spectral range obtained with off-line FT-IR.

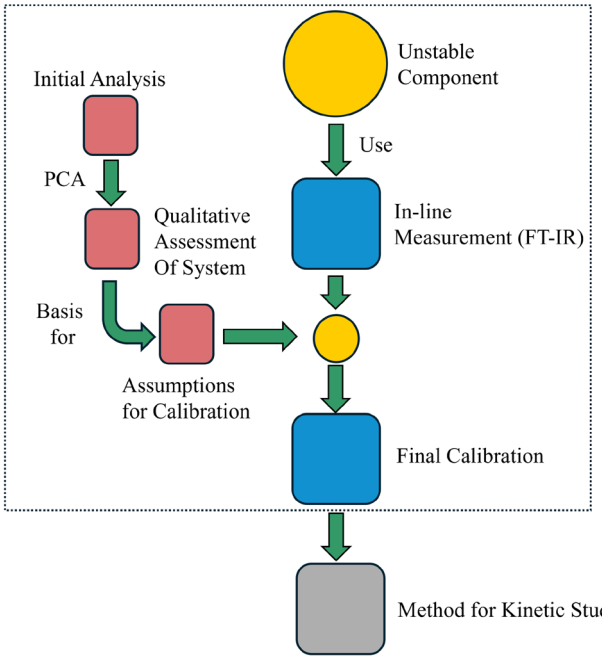

Fig. 4 The step-by-step calibration strategy followed in this work. The dotted box represents the scope of this work. The step from "assumptions for calibration" to "final calibration" is illustrated in more detail in Fig. 5.

In-line calibration of unstable components has been successfully performed in the literature with multivariate curve resoultion (MCR). This technique attempts to break down a set of (mixture) spectra into a linear combination of their pure component spectra, which may represent real pure component spectra. These pure component spectra can be used to calculate the concentrations of the pure component in newly measured mixture spectra as long as the spectroscopic signals are a linear response of their respective concentrations.[21,22] MCR has been previously successfully used to develop a (nearly) calibration-free evaluation tool for a range of reactions with unstable intermediates.[23–25] However, MCR did not lead to good calibration models in this work, as the spectra do not correlate linearly to the pure components, likely due to the nonlinear spectral effects of hydrogen bonding; for example due to the shifting equilibria between the acid monomer–dimer[18] and between the acid-amide dimer[26–28] over the course of the reaction.

To find a different approach for calibrating the system, a qualitative chemometric analysis of the system is performed with PCA, to gain a deeper understanding of the occurring reactions and the spectral response. The findings of this analysis are discussed in-depth in subsection 3.2. They serve as a

basis for justifiable assumptions on the general system and reaction behavior. The step from "assumptions for calibration" to "final calibration" in Fig. 4 is visualized with more detail in Fig. 5.

The amide content in the eight samples withdrawn during the calibration experiment could be determined off-line. The amount of ammonia supplied to the system during the calibration experiment was carefully controlled and recorded at every stage. Assuming that all free ammonia in the system reacts (see subsubsection 3.2.1), a mass balance could be formulated based on the general reaction scheme in Fig. 1; each molecule of ammonia can react with an acid to either amide or salt. This gives the mixture composition of the three compounds at the eight sampling points (Fig. 5). It is technically possible to perform a PLS calibration based on only the eight spectra at these sampling points. However, as expected, the quality of the calibration was not satisfactory (see ESI, Fig. S2†). Instead, the composition of the eight spectra at the sampling points was used as basis for the next step towards calibration. Together with assumptions on the slow formation of amide at a reaction temperature of 120 °C (subsubsection 3.2.2), a mass balance could be performed on the spectra close to the sampling point. This gives the mixture composition of the three compounds in all 187 spectra around the sampling points. A PLS calibration with these 187 spectra as input led to a satisfactory calibration quality. The calibration can be used to carry out in-depth kinetic studies of fatty acid ammoniation.

3.2 Qualitative description of the reaction system

In order to be able to carry out an in-line calibration following the general strategy presented in subsection 3.1, several assumptions have to be made, which are based on the qualitative analysis of the reaction system in this section.

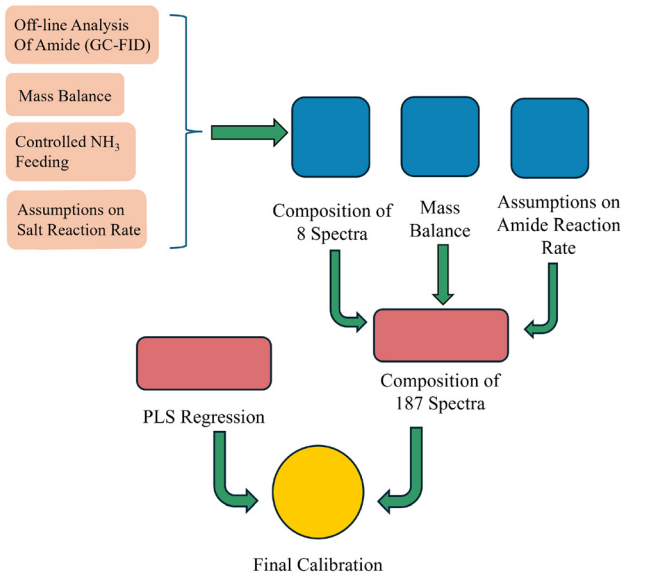

Fig. 5 Workflow from assumptions based on qualitative analysis of the system to calibration.

It is expected that the formation of ammonium salt from acid and ammonia as an acid–base reaction is very quick, and that the formation of amide and water from acid and ammonia is comparatively slow at 120 °C. To verify this, an experiment was performed as described in subsection 2.1; a total of 4.5 mol of ammonia was dosed step-wise to 7 mol oleic acid at 120 °C, to obtain a range of different mixtures of acid, salt and – especially at the later stages of the experiment – amide. Between each dosing step a 'reaction plateau' was applied, in which no ammonia was dosed and the system was left to react. The dosing steps of ammonia took about 5–10 min each, and the complete experiment 5 h. The raw FT-IR spectra obtained during this experiment are shown in Fig. 6a. The color gradient changes over the course of the reaction, the legend relates to the number assigned to each spectrum, taken every 16 s. Especially at later times (orange and yellow spectra), the formation of amide becomes apparent with the appearance of a peak at 1650 cm^{-1}.

3.2.1 Dosing of ammonia. The experiment can be divided into 'dosing steps' with ammonia addition and 'reaction plateaus' without ammonia addition. This section deals with the qualitative analysis of the 'dosing steps'.

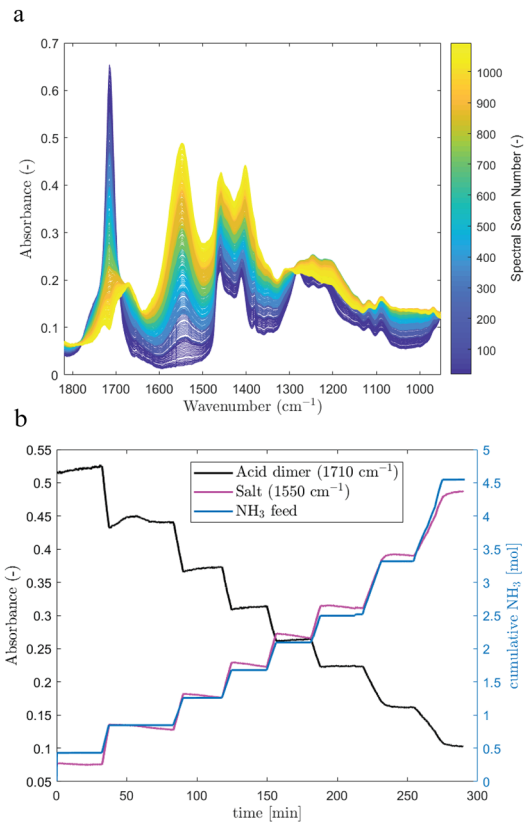

Fig. 6 Spectral response to stepwise dosing of ammonia to oleic acid at T = 120 °C. (a) Raw FT-IR spectra during 5 h of reaction, spectrum color represents the progression in time *via* the spectral scan number. (b) Cumulative ammonia feed and absorbance of acid at 1710 cm^{-1} and of salt at 1550 cm^{-1}. The cumulative ammonia dosing [mol] is represented on the right y-axis.

3.2.1.1 Acid–base reaction of ammonia and acid. The most immediate change observed in the spectra in Fig. 6a is the formation of salt from ammonia and acid. To illustrate the influence of the ammonia feed flow, the peak height of the absorbance of acid at 1710 cm^{-1} and of salt at 1550 cm^{-1} were plotted as a function of time alongside the cumulative dosed ammonia in Fig. 6b. This can be done without a calibration and serves to illustrate how quickly salt is formed from acid and ammonia. When ammonia is dosed, the acid band immediately drops, and the salt band immediately increases. This stops abruptly when the ammonia flow is turned off. During the reaction plateaus, the height of the salt band slightly decreases while the height of the acid band slightly increases – this is due to back-reaction of salt to acid and ammonia, and due to their further reaction towards amide.

During ammonia dosing, the formation of salt is so dominant that it overwhelms all other spectral changes. This can be visualized by performing a principal component analysis (PCA) on the spectra of the first dosing step. PCA allows for the reduction of the data set into a number of linear combinations, the principal components, that can explain the largest amount of variance of the original spectra.[29] The results of the PCA are shown in Fig. 8 and includes several spectra before and after the dosing as well.

The PCA results can be found in Fig. 8. The first principal component, PC1, explains 95.22% of the total spectral variance for the time around the first dosing step. The scores in Fig. 8 show that PC1 is proportional to the dosing of ammonia to the mixture over time (spectra index); the scores stay mostly flat, and then increase suddenly when ammonia is fed and once it is turned off, returns to a nearly flat line. The loadings in Fig. 8 (right) indicate that the main change is the simultaneous consumption of acid and formation of salt (band at 1550 cm^{-1}) and that the second principal component reflects only 0.18% of the spectral variance, mostly focusing on the change in monomer and dimer of the acid. This confirms the expectation that the addition of ammonia to the system causes immediate and quick consumption of the acid and simultaneous formation of the salt.

3.2.1.2 Concentration of dissolved water and ammonia. As shown in the previous section, nearly all added ammonia immediately reacts – to the salt and with a slower rate towards the amide. These three compounds are easily observed in the spectra from their characteristic bands. The other two components in the system, physically dissolved ammonia and the water formed alongside the fatty amide, are not directly visible in the spectra. Milella *et al.*[30] identified the IR band positions of H_2O, NH_3 and NH_4^+ in an aqueous liquid solution, which are assumed to be valid in an organic liquid solution as well. These positions are 1640 cm^{-1}, 1111 cm^{-1} and 1458 cm^{-1} for H_2O, NH_3 and NH_4^+ respectively. Max *et al.*[31] identified the band position of NH_3 at *ca.* 1100 cm^{-1}. These wavenumbers are investigated in Fig. 7 for spectral changes relating to H_2O, NH_3 and NH_4^+. The figure shows the first dosing step of ammonia to pure oleic acid, as well as the first 'reaction plateau' (visible in yellow), where ammonia dosing was stopped.

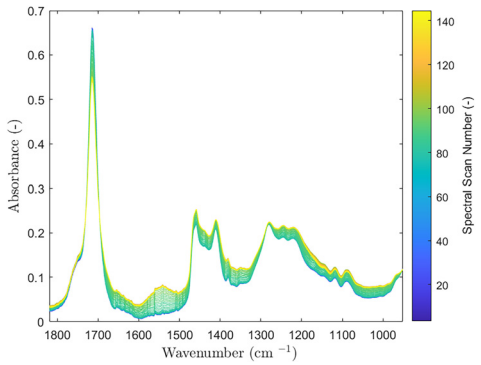

Fig. 7 Spectral change induced by dosing NH_3 to pure oleic acid at 120 °C. The change in color represents the spectral scan number (one every 16 s).

The pure oleic acid spectrum is visible in dark blue. The bands of physically dissolved water and NH_4^+ overlap with bands that are present in the oleic acid spectrum itself and are hard to distinguish. Considering NH_4^+ at 1458 cm^{-1}, it forms at the same time as the carboxylate as shown in the previous section; however, since the bands overlap with one of the oleic acid, its change cannot be distinguished from the carboxylate changing. Considering water, the temperature is 120 °C, water likely evaporates out of the liquid mixture into the vapor phase where it furthermore partially condenses at the poorly insulated reactor lid, leading to the water concentration in the liquid being likely close to zero. A band is present at *ca.* 1111 cm^{-1}, which increases during the dosing of ammonia and becomes stable once ammonia dosing is turned off. While this is at the correct spectral position for free ammonia, it cannot be related to free ammonia as it is also present in the pure oleic acid spectrum (dark blue). It is possible that this is a baseline effect. The free ammonia concentration in the reaction mixture is therefore nearly zero and small enough to not cause a visible spectral change even during ammonia dosing. Hence, free ammonia and water are not taken into account during the calibration.

3.2.2 Reaction towards amide. The previous section focused on the 'dosing steps' of the experiment described in subsection 3.2, while this section focuses on the 'reaction plateaus' without ammonia dosing. As the PCA in Fig. 8 shows, during dosing of ammonia, all other spectral changes are overwhelmed by the formation of salt. At 120 °C, the formation of amide is slow, therefore it is not visible during the comparatively short ammonia dosing times and overwhelmed by the energetically favored, exothermic formation of ammonium salt. Once ammonia dosing is stopped, salt formation stops instantly and other spectral changes become visible. This is exemplified for the first and the last reaction plateau in Fig. 9. The spectra of all reaction plateaus can be found in ESI S5.† The color change in the spectra represents the change over time; which shows there is little visible change. A plateau is about 20–30 min long, aside from the last plateau, which is 55 min long. Every ammonia addition in-between the plateaus

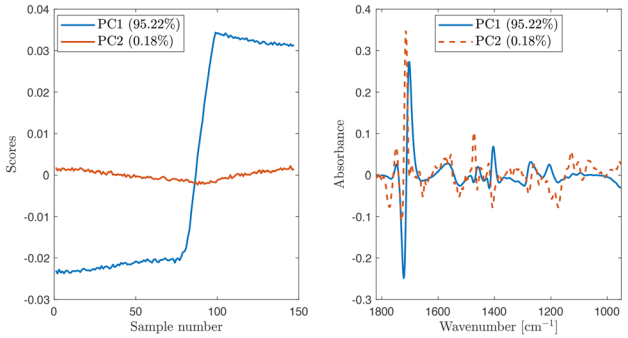

Fig. 8 PCA on the spectra of the first dosing step of ammonia. PC1 correlates with the ammonia dosing and explains 95.22% of all spectral variance. The data was pre-processed by taking its first derivative and mean centering.

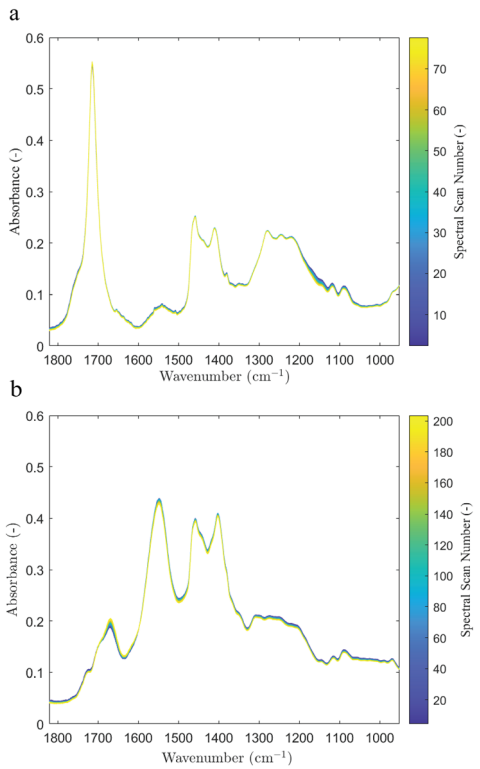

Fig. 9 Raw spectra of the (a) first and (b) last reaction plateau in-between ammonia dosing.

increases the salt band at 1550 cm^{-1} and decreases the acid band at 1710 cm^{-1}. The amide bands are covered by the acid and salt band, but especially during the later plateaus, the formation of amide can be clearly observed. During the plateaus, comparatively little spectral change can be observed, illustrating that the formation of amide is a slow reaction at 120 °C. The salt peak shrinks slightly, while the acid peaks shifts slightly to the right, showing formation of the amide. Some change is seen in the fingerprint region around 1200 cm^{-1} for both the first and the last reaction plateau. The first reaction plateau in Fig. 9a shows minor changes around 1750 cm^{-1}, indicating a shifting equilibrium between the acid monomer and dimer. The most obvious change can be seen for the last plateau in Fig. 9b around 1650 cm^{-1}, indicating the formation of amide, which was invisible during the dosing steps.

Before performing PCA, the spectra were pre-processed by smoothing the spectra, baseline correction and mean centering (see subsection 2.2). The PCA results are plotted in the relevant range in Fig. 10 exemplary for the first and the last reaction plateau. The PCA results for all plateaus can be found in ESI S5.†

The left column of Fig. 10 gives the PCA scores for each plateau. For each plateau, 2 or 3 principal components are the suggested amount, shown here are PCAs with 2 principal components, as the third component was usually comparatively minor. The principal component 1 is able to capture more than 87% of all spectral variance in all plateaus, and more than 90% in all but plateau 3: This PC1 increases more or less linearly over time (expressed by increasing spectral index, one every 16 s). Especially at the later reaction plateaus, the loadings show that PC1 captures mainly amide, indicating an approximately linear formation of amide over time, which was used for the estimation of the amide rate of formation in the ESI S4.†

The right column of Fig. 10 gives the loadings of the PCA for each plateau. The loadings of PC1 during the first plateau (Fig. 10b) resemble a spectrum containing a mixture of acid and amide with bands at *ca.* 1710 cm^{-1}, 1650 cm^{-1} and 1620 cm^{-1}. The "amide" contribution to the loadings of PC1

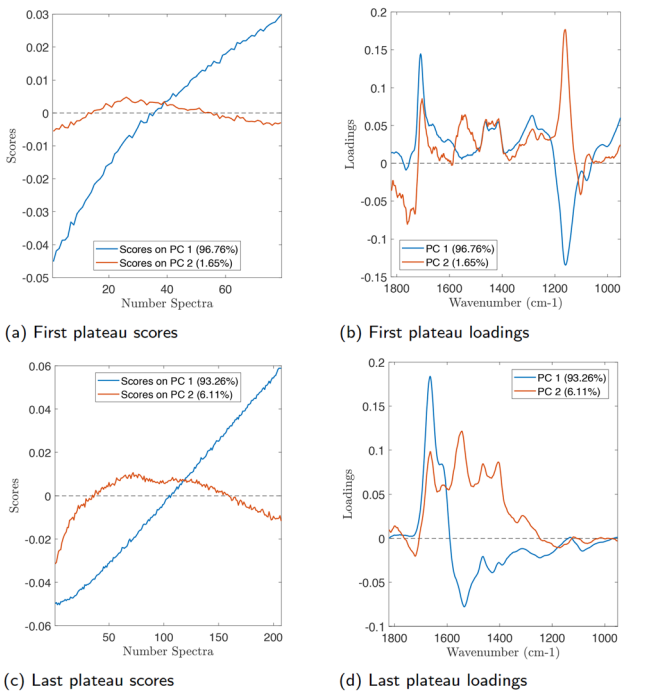

Fig. 10 PCA on the first and last reaction plateaus in-between ammonia dosing. The left column shows the PCA scores and the right column the corresponding loadings.

becomes more and more important over the course of each plateau, until the acid contribution is apparently vanished from the loadings in the last plateau (see Fig. 10d). At the later plateaus, the disappearance of the salt band is directly correlated with the appearance of amide in the loadings of PC1, see Fig. 10d.

This qualitative analysis of the FT-IR spectra gathered while step-wise dosing of ammonia to oleic acid at 120 °C demonstrates that the consumption of acid and the formation of salt are directly and immediately correlated to the dosing of the ammonia; the acid–base reaction is very fast and is strong enough to overwhelm any other spectral changes during dosing. Outside the dosing of ammonia, in the "plateaus", subtler spectral changes become more apparent: the most relevant is the slow formation of amide, which can be observed by principal component analysis as one of the most important spectral changes, and occurs slowly and approximately linearly.

3.3 Quantitative description of the reaction system

The next step after the qualitative description of the reaction system in the previous section is to quantify the composition of each of the reacting species. For this, the system has to be calibrated. According to the Beer–Lambert law, absorbance is linearly related to concentration. Without any other effects such as molecular interactions or temperatures changes, the mixture spectrum is a linear combination of the pure component spectra and their respective concentrations.[32]

Following the general strategy laid out in subsection 3.1, eight samples were taken during the calibration experiment described in paragraph 2.1.1.1, which is similar to the experiment discussed in the previous subsection 3.2, in which ammonia is dosed step-wise to fatty acid at 120 °C. The amide content in the samples can reliably be determined *via* GC (see Table S2†), but as the ammonium salt reverts back to acid at high temperatures, distinguishing between acid and salt with GC is not possible. As shown in subsubsection 3.2.1, the reaction of ammonia and acid towards salt is near instantaneous and the concentration of free ammonia in the system is close to zero. Therefore an assumption was made that all ammonia that was added to the system had reacted. Since the ammonia can only react to either amide or salt, a mole balance is employed alongside the amide content determined *via* GC to calculate the acid and salt content in the samples as shown in subsection 2.1.1.1. The compositions of the samples over time alongside the ammonia feed are given in Fig. 11a and in Table S3.† The spectra corresponding to these eight samples are given in their relevant spectral range in Fig. 11b.

Calibrating the system with eight samples gives unrealistic results, especially regarding the amide fraction; eight calibration points are too few to accurately capture the system's behavior. The number of calibration points could be increased by taking more physical samples, however, this is unpractical as preparation for sampling requires time due to the safety precautions necessary for working with the system. The safer option is to make assumptions on the system's behavior based on the qualitative analysis of the system in the previous

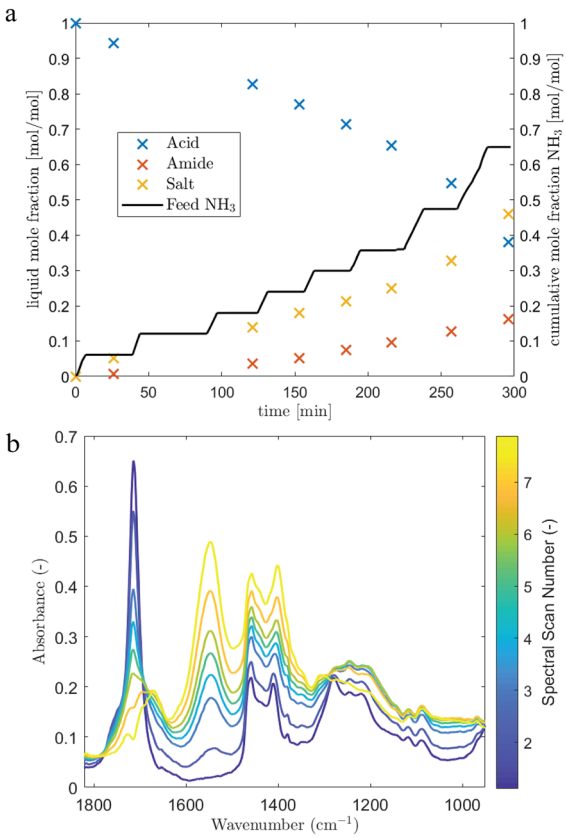

Fig. 11 Samples and spectra used for calibration, with amide content determined *via* GC-analysis and salt and acid content determined from a mole balance with the added cumulative ammonia feed. (a) Composition of samples taken during ammonia dosing and added cumulative ammonia. (b) Spectra corresponding to samples in relevant spectral range, color bar refers to spectral number (8 samples).

section, so that more spectra can be used for calibration. The concentration of physically dissolved ammonia, NH_3, in the reaction mixture, is constantly low and close to zero, even during the dosing period (see 3.2.1.2) as the formation of ammonium salt is rapid. In comparison, acid is present in excess. That indicates that the formation of amide from acid and free ammonia is limited by the ammonia concentration. The rate expression for the formation of amide can therefore be formulated using a pseudo-first order relationship.

$$\frac{dc_{amide}}{dt} = r_{amide} = k_{amide} \cdot c_{NH_3} = \text{const} \quad (3)$$

This means that the formation of amide is a linear process, which is also the case when looking at the behavior of the amide content over time in Fig. 11a. A linear function is fitted through the data in Fig. S4,† where it becomes apparent that this is a reasonable approximation. This relationship allows to calculate the amide content throughout the reaction despite the unknown exact value of the ammonia concentration.

The amide content can be calculated and the acid and salt content during the dosing steps can be computed from the mole balances in eqn (1) and (2). As the amide formation is not per-

fectly fitted by a linear function and as more complex spectral changes occur, the calculation of the acid, amide and salt content was only carried out for dosing steps which were close to a sampling point so that the amide concentration was reliable. For these dosing steps the content of acid, amide and salt were calculated and used for calibration. This increases the spectra available for calibration from 8 to 187, shown in Fig. 12.

The spectra are pre-processed by taking their first derivative and mean centering them, while the corresponding composition data was mean centered. A partial least squares regression (PLS) is carried out with PLS_Toolbox. PLS regression employs the idea of data reduction by computing latent variables (LV) similar to principal components in PCA, and combines it with a regression step linking the LV to a response variable of interest, such as the concentration of acid, amide and salt in this case. A PLS model with four LVs is developed based on the 187 spectra. The quality of the model and its predictive qualities are assessed by applying the model to (a) all 1112 spectra gathered during the calibration experiment and (b) a validation experiment as described in paragraph 2.1.1.2. The same experimental procedure was followed for the validation experiment; step-wise addition of ammonia to oleic acid at 120 °C. Only one sample was taken at the end of the reaction, as the number of points with a known acid content could be increased by closure of the mass balance following eqn (1). The comparison of the experimental composition (crosses) and the predicted concentrations (lines) for the calibration and the validation experiment are shown in Fig. 13. The circles represent the calculated acid content in the validation experiment based on the mole balance.

The prediction based on 187 calibration samples shows a similar general behavior for the composition profiles over time for both the calibration and the validation experiment, reflecting the similar nature of these experiments. The step-wise consumption of acid and formation of ammonium salt during ammonia dosing are clearly captured. The calibration experiment is predicted well, as is the prediction of the validation experiment. The acid content is overpredicted at the later reaction times of the validation experiment. A reason for this could

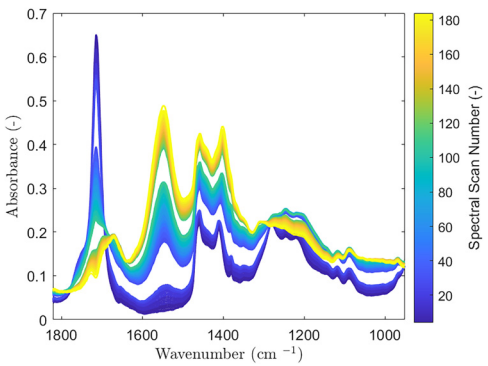

Fig. 12 187 spectra (samples and ammonia dosing steps) used for PLS calibration. Spectra are not pre-processed and shown in the relevant spectral range.

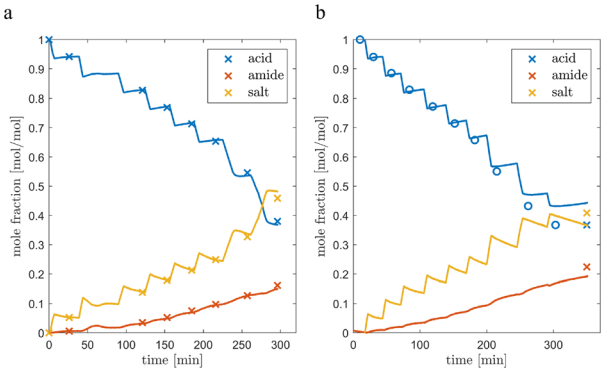

Fig. 13 PLS prediction of the calibration (a) and validation (b) experiment based on a PLS calibration of 187 spectra. Crosses denote experimental data points, lines the predicted compositions, circles the acid composition from a mass balance with the amount of ammonia dosed.

be inaccuracies in the data: calculating the composition of acid and salt by closing the mole balance with the added cumulative amount of ammonia means that the error of the ammonia mass flow meter (MFM) influences the quality of the prediction strongly. The effect the possible maximum error of the ammonia mass flow meter has on the measured ammonia mole flow is represented in Fig. S3.† The figure shows that the error of the MFM has more pronounced influences on the measured ammonia content and therefore the calibration at longer reaction times, as the error is also cumulative. The behavior of amide formation is overall realistic, as it shows a slow and steady, almost linear increase as suggested from the PCA in Fig. 10. The behavior of salt and acid during the reaction plateaus are similar to the plot of the peak heights without calibration in Fig. 6b. During a plateau, the salt content decreases over time, it reacts back to acid and ammonia. Consequently, the acid content increases over the course of a reaction plateau, but the slope of acid formation is lower than the slope of salt consumption. This can be explained by the formation of amide; some of the acid and ammonia react further to form amide and water. As some acid is formed during the plateau and its slope is not zero, the back reaction of salt to acid and ammonia is not rate-limiting for the formation of amide.

The quality of the calibration was assessed in a number of ways, firstly using a parity plot available in Fig. 14. Secondly, the error during the validation experiment is assessed by comparing the predicted and the observed acid composition. The observed acid concentrations come from the closing of the mass balance and the sample at the end of the reaction (as shown with circles and crosses in Fig. 13). The root mean square error (RMSE) of the acid concentration is calculated to 3.3mol%. Lastly, the quality is assessed with the root mean square error of calibration (RMSEC) and the root mean square error of cross validation (RMSECV), provided in Table 2, based on the PLS2 model for the 187 calibration samples. The RMSECV was calculated using random cross-validation with 10 splits and 5 iterations. The different assessment methods demonstrate the encouraging quality of the calibration.

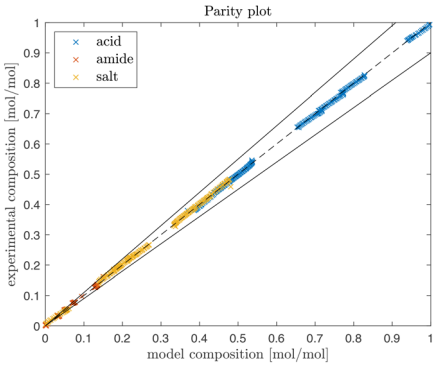

Fig. 14 Parity plot of the 187 sample spectra used for calibration and the modeled content based on the calibration. The black lines denote ±10% variation.

Table 2 Quality of calibration based on 187 samples assessed with RMSEC and RMSECV in mol%

Error	Acid	Amide	Salt
RMSEC	0.286	0.208	0.305
RMSECV	0.296	0.219	0.323

While the transferability of the calibration from one experiment to the other should be investigated with further validation experiments such as in Fig. 13, the quality of the prediction is encouraging considering the low number of samples taken and the assumptions taken that led to a good prediction of a complex reactive system that could only be calibrated in-line. Despite multiple reaction equilibria and the formation of unstable ammonium salt which prevent off-line calibration, a calibration could be developed based on a mole balance and eight samples analyzed with GC that can analyze the reaction with an error lower than 10% as shown with the parity plot.

4 Conclusion

This work measured the reaction of fatty acid and ammonia to salt or amide at 120 °C with in-line FT-IR analysis. The qualitative description of the system shows that the salt formation is near instantaneous and all ammonia is converted, first towards salt and later towards amide. The free ammonia concentration in the reaction liquid is found to be close to zero. The formation of salt and the consumption of acid is spectrally dominant during the addition of ammonia. Outside the addition of ammonia, the slower formation of amide becomes visible and proceeds in a nearly linear fashion as long as salt acts as a buffer that keeps the free ammonia concentration at the same, low value. It was shown that while ammonium salt decomposes to acid and ammonia at higher temperatures and therefore cannot be measured with GC-FID, the amide content in an off-line sample can be reliably determined through such a method. The amide content was determined for eight off-line samples, and the corresponding acid and salt contents through mass balance. Calculating an estimated rate of amide formation based on its near-linear rate of formation allows to use 179 more spectra for calibration, which resulted in a PLS-model with 4 LVs. The accuracy of the model was shown to have an error lower than 10% and was validated experimentally with a similar experiment. Further research could focus on exploring the transferability of the findings to a wider range of systems, such as those involving higher reaction temperatures. Moreover, the implementation of such a calibration stragety in a kinetic study can help develop more accurate models for the ammoniation of fatty acids. In summary, this work shows that gaining a deeper understanding of a reactive system at reaction conditions through chemometric analysis can facilitate the development of an in-line calibration and analysis method suitable for unstable reactants such as ammonium salt.

Author contributions

C. M. Raffel: conceptualization, methodology, validation, formal analysis, investigation, writing – original draft, writing – review & editing, visualization. J. Meekes: methodology, investigation, resources, validation. H.-J. van Manen: methodology, software, formal analysis, resources, data curation, writing – review & editing. A. J. B. ten Kate: conceptualization, writing – review & editing, supervision. A. Chaudhuri: writing – review & editing. J. van der Schaaf: conceptualization, supervision.

Conflicts of interest

The authors report no conflicts of interest in this study.

Data availability

The data supporting this article have been included as part of the ESI.†

Acknowledgements

This research was carried out within the HighSinc Program – a joint research initiative between Nouryon and the Department of Chemical Engineering and Chemistry from Eindhoven University of Technology.

References

1 B. Briscoe, V. Mustafaev and D. Tabor, *Wear*, 1972, **19**, 399–414.
2 B. Morris, *The Science and Technology of Flexible Packaging. Multilayer Films from Resin and Process to End Use*, Elsevier, Inc., 2022.

3 C. Swanson, D. Burg and R. Kleiman, *J. Appl. Polym. Sci.*, 1993, **9**, 226–238.
4 A. Corma, S. Iborra and A. Velty, *Chem. Rev.*, 2007, **107**, 2411–2502.
5 C. B. B. Farias, F. C. Almeida, I. A. Silva, T. C. Souza, H. M. Meira, R. D. C. F. Soares da Silva, J. M. Luna, V. A. Santos, A. Converti, I. M. Banat and L. A. Sarubbo, *Electron. J. Biotechnol.*, 2021, **51**, 28–39.
6 A. Chaudhuri, W. G. Backx, L. L. Moonen, C. W. Molenaar, W. Winkenweder, T. Ljungdahl and J. van der Schaaf, *Chem. Eng. J.*, 2021, **416**, 128962.
7 A. Mekki-Berrada, S. Bennici, J. P. Gillet, J. L. Couturier, J. L. Dubois and A. Auroux, *ChemSusChem*, 2013, **6**, 1478–1489.
8 Y.-H. Nagasaki, M. Tamura, M. Yabushita, Y. Nakagawa and K. Tomishige, *ChemCatChem*, 2022, **14**, e202101846.
9 H. Kita, W. Ozuka and G. Sugahara, *Kogyo Kagaku Zasshi*, 1956, **59**, 1047–1050.
10 F. Bizhanov, E. Yazbaev and Z. Prnazarov, *Izv. Akad. Nauk Gruz. SSR, Ser. Khim.*, 1985, **21**, 23–26.
11 H. Charville, D. A. Jackson, G. Hodges, A. Whiting and M. R. Wilson, *Eur. J. Org. Chem.*, 2011, 5981–5990.
12 W.-D. Hergeth, *Ullmann's Encycl. Ind. Chem.*, 2006, **25**, 345–397.
13 W. Chew and P. Sharratt, *Anal. Methods*, 2010, **2**, 1412–1438.
14 R. Chung and J. E. Hein, *Top. Catal.*, 2017, **60**, 594–608.
15 J. J. Max and C. Chapados, *J. Phys. Chem. A*, 2004, **108**, 3324–3337.
16 A. Filopoulou, S. Vlachou and S. C. Boyatzis, *Molecules*, 2021, **26**, 1–26.
17 M. Iwahashi, M. Suzuki, M. A. Czarnecki, Y. Liu and Y. Ozaki, *J. Chem. Soc., Faraday Trans.*, 1995, **91**, 697–701.
18 T. Genkawa, M. Watari, T. Nishii and M. Suzuki, *Appl. Spectrosc.*, 2013, **67**, 724–730.
19 H. Shurvell, *Handbook of Vibrational Spectroscopy*, 2006, pp. 1783–1816.
20 F. S. Parker, *Amides and Amines*, Springer US, Boston, MA, 1971, pp. 165–172.
21 J. Diewok, A. de Juan, M. Maeder, R. Tauler and B. Lendl, *Anal. Chem.*, 2003, 641–647.
22 S. Rutan, A. de Juan and R. Tauler, *Introduction to Multivariate Curve Resolution*, Elsevier B.V., Amsterdam, 2009, pp. 249–259.
23 V. Fath, N. Kockmann and T. Röder, *Chem. Eng. Technol.*, 2019, **42**, 2095–2104.
24 V. Fath, P. Lau, C. Greve, N. Kockmann and T. Röder, *Org. Process Res. Dev.*, 2020, **24**, 1955–1968.
25 I. Csontos, H. Pataki, A. Farkas, H. Bata, B. Vajna, Z. K. Nagy, G. Keglevich and G. J. Marosi, *Org. Process Res. Dev.*, 2015, **19**, 189–195.
26 S. R. Chaudhari and N. Suryaprakash, *J. Mol. Struct.*, 2012, **1016**, 163–168.
27 M. T. Huggins, N. T. Salzameda and D. A. Lightner, *Supramol. Chem.*, 2011, **23**, 226–238.
28 S. Saha and G. R. Desiraju, *J. Am. Chem. Soc.*, 2018, **140**, 6361–6373.
29 M. Greenacre, P. J. F. Groenen, T. Hastie, A. I. D'Enza, A. Markos and E. Tuzhilina, *Nat. Rev. Methods Primers*, 2022, **2**, 100.
30 F. Milella and M. Mazzotti, *React. Chem. Eng.*, 2019, **4**, 1284–1302.
31 J. J. Max and C. Chapados, *J. Mol. Struct.*, 2013, **1046**, 124–135.
32 S. Wold, M. Sjöström and L. Eriksson, *Chemom. Intell. Lab. Syst.*, 2001, **58**, 109–130.